AIP | Journal of Applied Physics

Substrate orientation dependence on the solid phase epitaxial growth rate of Ge

B. L. Darby, B. R. Yates, I. Martin-Bragado, J. L. Gomez-Selles, R. G. Elliman et al.

Citation: J. Appl. Phys. **113**, 033505 (2013); doi: 10.1063/1.4776718
View online: http://dx.doi.org/10.1063/1.4776718
View Table of Contents: http://jap.aip.org/resource/1/JAPIAU/v113/i3
Published by the American Institute of Physics.

Substrate orientation dependence on the solid phase epitaxial growth rate of Ge

B. L. Darby,[1,a)] B. R. Yates,[1] I. Martin-Bragado,[2] J. L. Gomez-Selles,[2] R. G. Elliman,[3] and K. S. Jones[1]
[1]*Department of Materials Science and Engineering, University of Florida, Gainesville, Florida 32611-6400, USA*
[2]*IMDEA Materials Institute, Erik Kendel 2, Parque cientifico tecnologico, 28906 Getafe, Madrid, Spain*
[3]*Department of Electronic Materials Engineering, Research School of Physical Sciences and Engineering, Australian National University, Canberra, Australian Capital Territory 0200, Australia*

(Received 23 October 2012; accepted 28 December 2012; published online 15 January 2013)

The solid phase epitaxial growth process has been studied at 330 °C by transmission electron microscopy for Ge wafers polished at 10°–15° increments from the [001] to [011] orientations. The velocity showed a strong dependence on substrate orientation with the [001] direction displaying a velocity 16 times greater than the [111] direction. A lattice kinetic Monte Carlo model was used to simulate solid phase epitaxial growth (SPEG) rates at different orientations, and simulations compared well with experimental results. Cross sectional transmission electron microscopy and plan view transmission electron microscopy revealed stacking fault and twin defect formation in the [111] orientation where all other orientations showed only hairpin dislocations. The twin defects formed from Ge SPEG were comparatively less dense than what has previously been reported for Si, which gave rise to higher normalized velocities and a constant [111] SPEG velocity for Ge. © *2013 American Institute of Physics*. [http://dx.doi.org/10.1063/1.4776718]

I. INTRODUCTION

Amorphization caused by ion implantation and subsequent solid phase epitaxial growth (SPEG)[1] is a common technique used to dope the source and drain regions of field effect transistors (FETs).[2] With the renewed interest in Ge as an alternative material in complementary metal-oxide-semiconductor devices,[3–6] it is important to understand the recrystallization process and defects that form for this material. The SPEG orientation dependence for Si has been well studied, but relatively little knowledge is known for Ge. The SPEG process for Si shows a clear dependence on orientation where the regrowth in the [001] direction is about 25 times greater than the [111] and about 3 times greater than the [011].[7–10] It is believed that the difference in SPEG rate is attributed to the number of amorphous atoms at the amorphous crystalline (α-c) interface that are needed to attach to a crystalline atom with 2 undistorted bonds. This number is 1, 2, and 3 for [001], [011], and [111], respectively.[11,12] It is also theorized that twin defect formation affects SPEG. Csepregi *et al*. have noted high defect densities within 16° of the [111] orientation for Si,[9,13] and Monte Carlo simulations match reasonably well with the experiments.[12]

The orientation dependence of SPEG has been measured from [001] to [011] for Si, but so far only 3 relative velocities along the major indices have been reported for Ge.[9,10] This study reports the SPEG orientation dependence for Ge and characterizes the resulting defect structures upon crystallization. It also compares the SPEG process of Ge with past work done for Si.

II. EXPERIMENTAL

(001) Ge wafers with a resistivity of 0.02 Ω cm and (011) Ge wafers with a resistivity of 56 Ω cm were implanted with 1×10^{15} Ge^+/cm^2 at 1 MeV using a 5SDH-4 tandem accelerator at the Australian National University. The low background doping ($<1 \times 10^{17}$ As/cm^3) for these Ge wafers was not expected to affect SPEG velocities in this experiment.[14] A set of (001) Ge wafers were mounted on a polishing stub at angles of 15°, 25,° 40,° 54.7,° 70,° and 80° away from the [001]. The samples were then mechanically polished to a mirror finish, and the entire stub was implanted at 0°. In this way, the polished surface was normal to the ion beam during implant. For all samples, this implant resulted in a continuous amorphous layer extending approximately 800 nm from the surface. The samples were then annealed in a tube furnace with flowing N_2 at 330 °C, and the amorphous layer thicknesses were measured at various times via cross-sectional transmission electron microscopy (XTEM). Plan-view transmission electron microscopy (PTEM) was also used to characterize and quantify defect formation of the fully recrystallized structures for all orientations. An FEI DB235 focused ion beam (FIB) was used to prepare both XTEM and PTEM samples. A JEOL 2010 F microscope operated at 200 kV was used for imaging XTEM samples, while a JEOL 200CX microscope operated at 200 kV was used for imaging PTEM samples.

III. SIMULATIONS

The lattice kinetic Monte Carlo (LKMC) code MMonCa was used adapting existing implementations to Ge recrystallization.[13] The parameters used are listed in Table I. Formation of twin defects was properly accounted, and its

a)Author to whom correspondence should be addressed. Electronic mail: bdarby@ufl.edu.

TABLE I. Recrystallization parameters used in this work.

Configuration	Prefactor(atoms/s)
$K(100_h)$	2.35×10^{18}
$K(100_l)$	1.18×10^{17}
K(110)	2.41×10^{16}
K(111)	1.50×10^{12}

configuration was introduced in the simulation. The lateral cell size for the simulation was 180×20 nm^2 with a SPEG growth of 21 nm in the x direction. The activation energy used for Ge SPEG in this model was 2.17 eV.

IV. RESULTS

Fig. 1 shows an XTEM annealing sequence of the SPEG process for (001) Ge (0°). The distance from the surface to the α/c interface marks the thickness of the amorphous layer. The regrowth of the amorphous layer was then measured at 330 °C in this fashion for all 8 orientations.

Fig. 2 shows XTEM images for an isochronal 11 h anneal at 330 °C for all 8 orientations studied in this work. The difference in amorphous layer thickness clearly illustrates a SPEG dependence on substrate orientation. No significant difference in roughness of the α/c interface was observed among the 8 orientations, which is indicative of low defect concentrations. This is unique to Ge since an increase in interface roughness was observed for [111] Si relative to other Si orientations.[8]

The regrowth for the 3 main orientations ([001], [111], and [011]) is graphed in Fig. 3. The [001] velocity for this work was measured to be 1.05 nm/min at 330 °C, which was 16 times faster than the [111] velocity, and 1.4 times faster than the [011] velocity. Unlike Si, which exhibited a bimodal growth regime for the [111], the SPEG velocity for [111] Ge was constant throughout the annealing sequence.[8,9] XTEM analysis revealed the presence of small microtwins and stacking faults parallel to the (111) surface for the 54.7° oriented samples only. These defects were 10–20 nm long and typically less than 10 monolayers thick. The constant SPEG velocity in the [111] is likely a reflection of the constant twin and stacking fault concentration throughout the regrown layer observed in the XTEM image of Fig. 4(a). A high resolution XTEM image of a stacking fault parallel to the surface is shown in Fig. 4(b). The fast Fourier transform (FFT) in Fig. 4(b) shows streaking in the diffraction pattern, which is characteristic of stacking faults.[15]

In order to quantify defect formation for the Ge samples, PTEM samples were made for all 8 orientations. Anneal times were chosen based on each orientation's SPEG velocity in order to image the fully or near-fully recrystallized structures. Figures 5(a)–5(c) show PTEM images of the [001], [111], and [110] regrown layers, respectively. Hairpin

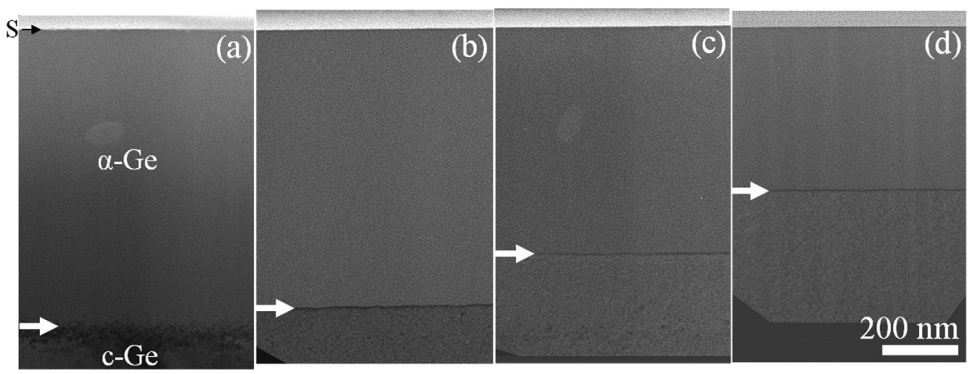

FIG. 1. XTEM micrographs of an annealing sequence at 330 °C of the 0° [001] Ge orientation. Sample was implanted at 1 MeV with 1×10^{15} Ge^+/cm^2 (a) and annealed for 30 min (b), 150 min (c), and 330 min (d). The white arrows indicate the location of the α/c interface.

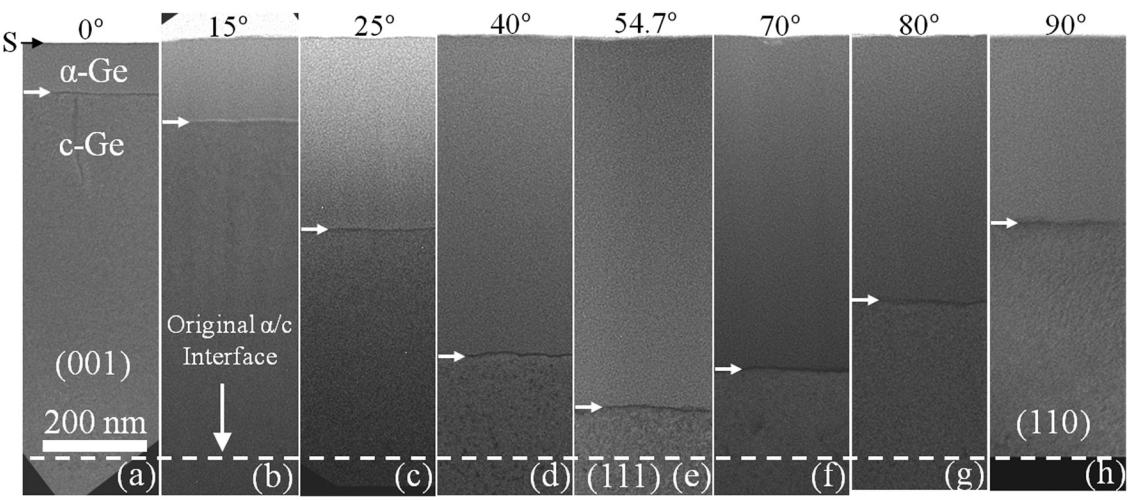

FIG. 2. An isochronal anneal for all 8 orientations done at 330 °C for 11 h. The [111] direction is noticeably the slowest velocity, while [001] is the fastest. The orientations are 0° (a), 15° (b), 25° (c), 40° (d), 54.7° (e), 70° (f), 80° (g), and 90° (h).

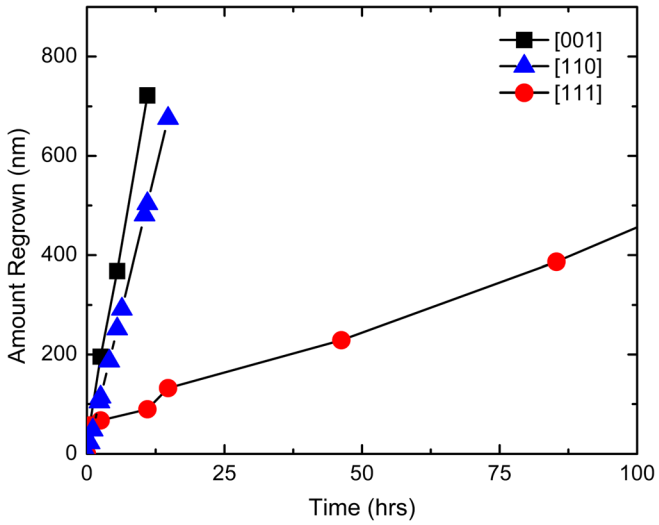

FIG. 3. Plot of regrowth over time at 330 °C for the 3 main orientations in Ge: [001] (0°), [111] (54.7°), and [110] (90°).

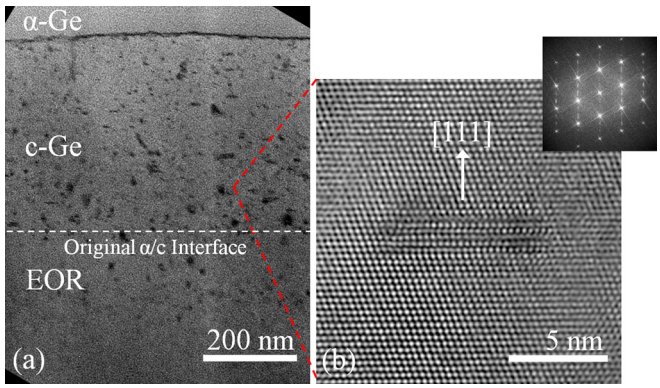

FIG. 4. XTEM images of (111) Ge annealed at 330 °C for 85 h. A low magnification image of the partially recrystallized layer (a) and a high resolution image of the stacking faults parallel to the surface with an FFT showing streaking (b).

dislocations were observed within the recrystallized layers for all 8 Ge orientations with an average density of $2.7 \times 10^8 \pm 1.6 \times 10^8\,\mathrm{cm}^{-2}$. These defects nucleated at the α-c interface where pockets of amorphous material recrystallized at a slightly different orientation than the substrate.[16] This is common for high energy implants (1 MeV), which produce a rough α-c interface.[17] It is not surprising that similar hairpin concentrations existed among the samples since each had the same implant and presumably the same α-c interface morphology.

In addition to hairpin dislocations, large stacking faults and twins were observed on inclined {111} planes for the 54.7° orientation only, as seen in Fig. 5(b). For Si substrates, Csepregi *et al*. noticed a high concentration of defects within 16° of the [111] axis,[9] but this was not the case for Ge. Both XTEM and PTEM analyses confirmed that these large stacking faults and twins lie on inclined {111} planes. The density of these defects was only $\sim 1 \times 10^8\,\mathrm{cm}^{-2}$ and was not great enough to produce twin spots in diffraction, as seen in Si.[18] A burgers vector analysis was performed by tilting to different g vectors such that $\mathbf{g} \times \mathbf{b} = 0$ was satisfied. By tilting to 3 unique g vectors which satisfied this criterion, the fault vector for the defects on inclined {111} planes was determined to be of a/6{211} type, where "a" is the lattice constant of Ge (0.565 nm). The density of the smaller stacking faults that were parallel to the (111) surface was unable to be resolved due to their limited diffraction contrast in PTEM.

A linear regression analysis was performed for the measured SPEG velocities, and the results are shown in Fig. 6. The α/c interface planarized after the first anneal (30 min) for all samples, resulting in a period of enhanced SPEG velocity. The linear regression was thus applied after this planarization step to reduce error in the calculations. The SPEG velocities were measured at 330 °C, and the data in Fig. 6 represent measurements from nearly 50 XTEM images over the 8 orientations. Ge SPEG was then modeled as a function of substrate orientation with LKMC.

Fig. 7 shows the SPEG velocities for Ge compared with literature values for Ge and Si normalized to the [001] direction. Due to the difference in activation energies between Si and Ge, the recrystallization temperature for Si was 550 °C. Overall, the normalized Ge velocities are higher than those in Si. The normalized Ge velocities matched reasonably well with the literature values measured at 331.5 °C.[7,10] The absolute velocities, however, differed by a factor of 3, which is likely due to temperature calibration errors. The absolute velocities from other literature reports match well with the present work, validating the results.[19–21]

V. DISCUSSION

The use of TEM in this work offered the advantage to measure SPEG velocity as well as defect concentration. This allowed for correlating a structure property relationship for Ge SPEG. While hairpin dislocations were observed for all orientations, their density did not vary significantly among the orientations. Elghor *et al*. have shown that hairpin concentrations of $\sim 1 \times 10^{11}\,\mathrm{cm}^{-2}$ can cause a 30% reduction in

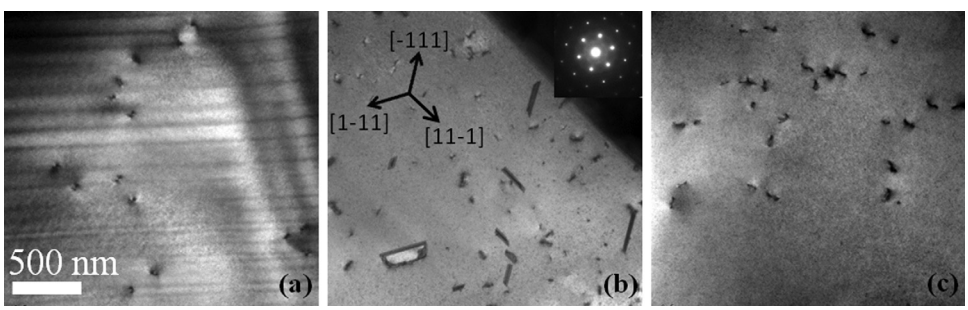

FIG. 5. PTEM images of fully recrystallized samples annealed at 330 °C. (a) [001] Ge annealed for 11 h, (b) [111] Ge annealed for 7.5 days with a selected area diffraction inset, and (c) [011] Ge annealed for 20.3 h.

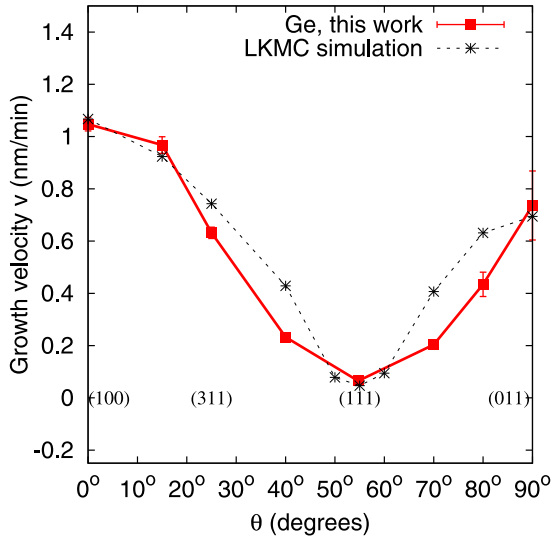

FIG. 6. Measured SPEG velocities for Ge at different orientations with LKMC simulations. Anneal temperature was 330 °C.

SPEG rate,[16] but this density is roughly 3 orders of magnitude larger than what was observed in this work. Moreover, the [001] SPEG velocity compared well with previous SPEG experiments in Ge, where no hairpin dislocations were observed.[22] This evidence supports the conclusion that the low density of hairpin dislocations did not contribute to the orientation dependence on SPEG for this work.

Previous studies have shown 2 velocity regimes for Si [111], where the initial 150 nm of SPEG is 3 times slower than the remaining growth.[7–9] This was attributed to a high density of small twins near the initial α-c interface, followed by a lower density of larger twins near the surface.[18] In contrast, only one [111] velocity existed for Ge. This is likely due to the low density of defects on {111} planes in Ge. The density of inclined stacking faults and twins in this work was estimated to be $\sim 1 \times 10^{13}\,\mathrm{cm}^{-3}$ (assuming a sample thickness of 200 nm), where the density in Si was reported as high as $\sim 1 \times 10^{16}\,\mathrm{cm}^{-3}$.[18] It follows that a lower density of stacking faults and twins could lead to a less evident change in the [111] SPEG velocity. It could also be that the transition between the phases occurred so rapidly that it was not observed or not great enough to produce an appreciable change in velocity.

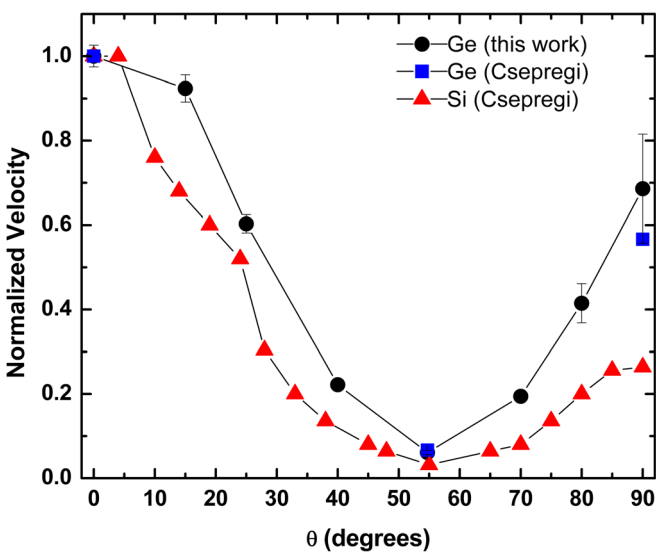

FIG. 7. SPEG velocities normalized to the [001] direction for Ge in this work compared with normalized literature values for Ge and Si. Csepregi used RBS to measure SPEG velocities for Si at 550 °C and Ge at 331.5 °C.[9,10]

Recent theories have suggested that the SPEG velocity for orientations close to the [111] is limited by the formation of twin defects.[12,23] Compared with Si, this work showed a smaller concentration of defects for Ge in such orientations.[18] The higher normalized SPEG velocities near the [111] seem to confirm this theory. Thus, it is likely that the geometrical effect of amorphous atoms bonding at the interface controls the overall shape of the orientation dependence in Fig. 7, while twin defect concentration influences the degree of curvature around the [111] orientations. Since Ge has smaller concentrations of twins than Si, the normalized velocities are higher than those in Si.

The reason for decreased defects in Ge compared with Si could stem from a difference in stacking fault energies. First principles calculations have shown that the stacking fault energy of Si ranges from 26 to 33 mJm^{-2}, while Ge is 46–56 mJm^{-2}.[24] The larger stacking fault energy means that the defect would be harder to form, which correlates well with experimental results.

VI. CONCLUSIONS

The solid phase epitaxial growth process has been studied at 330 °C by TEM for Ge wafers polished to various orientations. The velocity showed a strong dependence on substrate orientation with the [001] direction displaying a velocity 16 times greater than the [111] direction. A lattice kinetic Monte Carlo model was used to simulate SPEG rates at different orientations and simulations compared well with experimental results. PTEM revealed stacking fault and twin defect formation in the [111] orientation where all other orientations showed only hairpin dislocations. The twin defects formed from Ge SPEG were comparatively less dense than what has previously been reported for Si, and unlike Si, Ge [111] SPEG showed a constant SPEG velocity throughout the entire annealing sequence. The structural results indicated that low defect densities on {111} planes gave rise to higher normalized SPEG velocities for Ge compared to Si. The decreased defect densities in Ge could result from a larger stacking fault energy compared with Si.

ACKNOWLEDGMENTS

The authors acknowledge Intel Corporation for funding this work. I.M.-B. acknowledges funding from the European project MASTIC (PCIG09-GA-2011-293783). The Major Analytical Instrumentation Center at the University of Florida is acknowledged for use of the focused ion beam and transmission electron microscope facilities. The machine shop of the Chemistry Department at the University of Florida is acknowledged for making the polishing chuck for this experiment. We also acknowledge support from the

Australian Government's NCRIS/EIF funding programs for access to Heavy Ion Accelerator Facilities at the Australian National University.

[1]G. Q. Lu, E. Nygren, and M. J. Aziz, J. Appl. Phys. **70**, 5323 (1991).
[2]A. Bousetta, J. A. van den Berg, D. G. Armour, and P. C. Zalm, Appl. Phys. Lett. **58**, 1626 (1991).
[3]A. Satta, E. Simoen, T. Clarysse, T. Janssens, A. Benedetti, B. De Jaeger, M. Meuris, and W. Vandervorst, Appl. Phys. Lett. **87**, 172109 (2005).
[4]E. Simoen, A. Satta, A. D'Amore, T. Janssens, T. Clarysse, K. Martens, B. De Jaeger, A. Benedetti, I. Hoflijk, B. Brijs, M. Meuris, and W. Vandervorst, Mater. Sci. Semicond. Process. **9**, 634 (2006).
[5]D. Kuzum, A. J. Pethe, T. Krishnamohan, and K. C. Saraswat, IEEE Trans. Electron Devices **56**, 648 (2009).
[6]C. O. Chui, K. Gopalakrishnan, P. B. Griffin, J. D. Plummer, and K. C. Saraswat, Appl. Phys. Lett. **83**, 3275 (2003).
[7]K. T. Ho, I. Suni, and M.-A. Nicolet, J. Appl. Phys. **56**, 1207 (1984).
[8]L. Csepregi, J. W. Mayer, and T. W. Sigmon, Appl. Phys. Lett. **29**, 92 (1976).
[9]L. Csepregi, E. F. Kennedy, J. W. Mayer, and T. W. Sigmon, J. Appl. Phys. **49**, 3906 (1978).
[10]L. Csepregi, R. P. Kullen, J. W. Mayer, and T. W. Sigmon, Solid State Commun. **21**, 1019 (1977).
[11]I. Martin-Bragado and V. Moroz, Appl. Phys. Lett. **95**, 123123 (2009).
[12]I. Martin-Bragado, Scr. Mater. **66**, 186 (2012).
[13]I. Martin-Bragado and B. Sklenard, J. Appl. Phys. **112**, 024327 (2012).
[14]B. C. Johnson, T. Ohshima, and J. C. McCallum, J. Appl. Phys. **111**, 034906 (2012).
[15]D. B. Williams and C. B. Carter, *Transmission Electron Microscopy: A Textbook for Materials Science*. *Spectrometry* (Plenum, 1996).
[16]M. K. Elghor, O. W. Holland, C. W. White, and S. J. Pennycook, J. Mater. Res. **5**, 352 (1990).
[17]K. S. Jones, S. Prussin, and E. R. Weber, Appl. Phys. A: Mater. Sci. Process. **45**, 1 (1988).
[18]M. D. Rechtin, Philos. Mag. A **37**, 605 (1978).
[19]A. Claverie, S. Koffel, N. Cherkashin, G. Benassayag, and P. Scheiblin, Thin Solid Films **518**, 2307 (2010).
[20]T. E. Haynes, M. J. Antonell, C. A. Lee, and K. S. Jones, Phys. Rev. B **51**, 7762 (1995).
[21]B. C. Johnson, P. Gortmaker, and J. C. McCallum, Phys. Rev. B **77**, 214109 (2008).
[22]B. L. Darby, B. R. Yates, N. G. Rudawski, K. S. Jones, and A. Kontos, Nucl. Instrum. Methods Phys. Res. B **269**, 20 (2011).
[23]I. Martin-Bragado, Appl. Phys. Lett. **98**, 233109 (2011).
[24]P. J. H. Denteneer and W. van Haeringen, J. Phys. C **20**, L883 (1987).